5.1   **AN IMPROVED METHOD TO REPRESENT AVIATION EMISSIONS IN AIR QUALITY
MODELING SYSTEMS AND THEIR IMPACTS ON AIR QUALITY**

Saravanan Arunachalam,* Bok H. Baek, Binyu Wang, Neil Davis, Andrew Holland,
Zachariah Adelman, Uma Shankar, Francis Binkowski, and Adel Hanna
Institute for the Environment, The University of North Carolina, Chapel Hill, NC

Ted Thrasher and Philip Soucacos
CSSI, Inc., Washington, D.C.

1. INTRODUCTION

Emissions from aviation sources typically represent a small portion of the total emissions in an air quality region. However, given the projected demand for aviation capacity and the continued decrease of emissions from most other anthropogenic sources, the analysis of emissions from aviation is of increased importance to understand their impacts on air quality. The Federal Aviation Administration (FAA) Emissions and Dispersion Modeling System (EDMS) (Federal Register, 1998) is the required model for performing air quality analysis of aviation sources in the United States and is typically used to analyze changes to local air quality in the vicinity of individual airports. In the public release, EDMS computes spatially and temporally allocated emissions for use with the American Meteorological Society/U.S. EPA Regulatory Model (AERMOD) for estimating pollutant concentrations. The EPA National Emissions Inventory (NEI) that is currently used to support local- and regional-scale air quality modeling represents aircraft as surface-level emissions by county.

Given that aviation sources, and their emissions, operate in a three-dimensional (3-D) environment, air quality models would benefit from emissions data that are more realistically spatially allocated. To provide realistic 3-D representations of all aviation emissions, we developed an interface to the Sparse Matrix Operator Kernel Emissions (SMOKE) modeling system (Houyoux et al., 2000; Baek et al., 2006) called EDMS2Inv that accepts the AERMOD-ready spatially and temporally allocated (hourly) emissions inventory from EDMS for direct use in the Community Multiscale Air Quality (CMAQ) model (Byun and Ching, 1999; Byun and Schere 2006; CMAQ, 2008). We provide an overview of the implementation of this improved representation of aviation emissions from three airports (Atlanta–Hartsfield, Chicago–O'Hare and Providence–T.F. Green) using the new link from EDMS to CMAQ, and discuss results from annual CMAQ simulations with an emphasis on the contribution of aircraft emissions below 10,000 feet to PM$_{2.5}$ predictions.

2. EDMS2INV SMOKE INTERFACE

Since 1998, FAA's EDMS has been the required mode for assessing the air quality impacts of airport emission sources, which consist of aircraft, auxiliary power units (APUs), ground support equipment (GSE), ground access vehicles, and stationary sources. EDMS interfaces with AERMOD version 07026 (U.S. EPA, 2004; Cimorelli, 2005) and its supporting weather and terrain processors, AERMET version 06341 and AERMAP version 06341. EDMS (EDMS, 2007) can be used as part of an air quality assessment conducted using AERMOD, or it can be applied to simply generate emission inventories. Currently, EDMS estimates emissions of total hydrocarbons (THC), nonmethane hydrocarbons (NMHC), volatile organic compounds (VOC), CO, oxides of nitrogen (NO$_x$), oxides of sulfur (SO$_x$), and particulate matter of size less than 10 and 2.5 μm (PM$_{10}$ and PM$_{2.5}$) in aerodynamic diameter. EDMS also includes GSE emission factor data from EPA's NONROAD model (U.S. EPA, 2005), and an interface to EPA's MOBILE version 6.2 (U.S. EPA, 2003) for obtaining on-road vehicle emission factors. Aircraft activity in EDMS is expressed in terms of landing/takeoff (LTO) cycles, which include startup, taxiing, queuing, takeoff, climb-out, and approach.

We developed a research version of EDMS for this study to estimate emissions of criteria pollutants from commercial aviation activities from the ground level up to 10,000 ft. In the public release, EDMS uses a detailed vertical two-dimensional grid below 1,000 feet. However, in order to improve the computer run time, the model collapses aircraft sources between 1,000 feet and the mixing height into a plane (level) located halfway between those two altitudes. The research version of EDMS uses a vertical structure that is consistent with the chosen CMAQ application from the surface to 10,000 ft. EDMS uses AERMOD for air pollutant dispersion; however, the dispersion modeling component within EDMS was not used for this study.

To provide realistic representations of all emissions from aviation and airport-related sources, we developed EDMS2Inv (Baek et al., 2007), an interface to the SMOKE modeling system, to process hourly emission inventory outputs from the EDMS to create emissions inputs to CMAQ. This interface allows enhanced representation of emission inputs from aviation sources in air quality models, and can help in designing new sensitivity scenarios to assess the impacts of the rapid growth of aviation. The primary objective of this interface is to convert the EDMS output (which has historically been used only by AERMOD) to provide an inventory format for SMOKE to ensure that aviation emissions are processed correctly. We also enhanced SMOKE to compute emissions layer fractions so that these aircraft emissions can be distributed into the appropriate model layers aloft.

Corresponding author address: Saravanan Arunachalam, Institute for the Environment, UNC-Chapel Hill, 137 E. Franklin St #656, CB 6116, Chapel Hill, NC 27599-6116; e-mail: sarav@unc.edu.

This study focuses on three airports: Atlanta – Hartsfield (ATL), Chicago – O'Hare (ORD), and Providence – T.F. Green (PVD). These were chosen based upon the availability of existing Environmental Impacts Statements (EISs). EDMS estimates of criteria air pollutants (CAPs) from commercial aircraft sources at these three airports were processed through the SMOKE model and then merged with the baseline emissions (with no aviation emissions) for subsequent modeling in CMAQ. The modeled contributions of aircraft emissions to background air quality can then be used for health risk exposure analysis.

For this study, EDMS emissions were generated for the three airports. Speciated $PM_{2.5}$ emissions were available for primary sulfate (PSO4), primary elemental carbon (PEC), and primary organic carbon (POC). The $PM_{2.5}$ speciation is based upon the First-Order Approximation (FOA) Version 3.0a (FOA3a), which was developed by John Kinsey (EPA ORD) and Roger Wayson (FAA Volpe) to predict PM from commercial aircraft engines. FOA3a is a conservative extension of the Committee on Aviation Environmental Protection (CAEP)'s approved FOA3 (ICAO, 2007). Table 1 shows the annual emissions at the three airports for key criteria pollutants, along with the breakdown of $PM_{2.5}$ into its speciated components. Although EDMS can estimate emissions for all of the source types that are found at airports, this analysis included only the emissions from the main engines of commercial aircraft. We included 73 commercial aircraft types for ATL, 109 for ORD, and 144 for PVD.

Species	ATL	ORD	PVD
NO_x	7,748	7,453	562
SO_x	815	774	56
$PM_{2.5}$	175	170	12
PSO4	34.6%	34.8%	34.2%
PEC	49.6%	48.7%	48.7%
POC	14.8%	16.5%	17.1%

Table 1. Aircraft emissions in short tons/year, and the breakdown of $PM_{2.5}$.

The CMAQ model application has a varying vertical resolution from the surface to 50 millibars (about 18 km). There are a total of 22 layers, with the first 15 layers spanning 10,000 ft, where aircraft emissions are provided. Table 2 shows the vertical structure of the modeling domains. The variation aloft of the emissions of $PM_{2.5}$, total hydrocarbons (THC), CO, and oxides of nitrogen (NO_x) for a typical day are shown for the Atlanta – Hartsfield airport in Figure 1.

To show the significant spatial enhancement in the vertical representation of aviation emissions in the vicinity of the airports during the LTO cycle in modeling systems, we present a vertical cross-section plot of $PM_{2.5}$ near the location of ATL airport, in the modeling domain's vertical structure. By enhancement, we are referring to the current general practice of representing all airport emissions in the model's surface layer. In Figure 2, each grid cell in the x-axis represents a 36-km grid cell, and each grid-cell in the y-axis represents a layer number (recall that layers have varying thicknesses [Table 2]). Figure 2 shows that while most of the emissions of all species are in the surface layer, there is a significant distribution of emissions in layers aloft. One can also see that in the top layers, emissions are at least two to three 36-km grid cells away from the grid cell where the airport is located, showing the path of aircraft as they approach or leave the airport during the LTO cycle.

Layer Number	Layer Top (m)
15	3090
14	2560
13	2110
12	1720
11	1380
10	1090
9	844
8	637
7	468
6	334
5	227
4	145
3	89
2	48
1	21

Table 2. CMAQ vertical structure (lowest 15 layers).

The airport layout was defined using the information provided by the FAA's National Aeronautical Charting Office (NACO), and the commercial aircraft operations were obtained from previous EIS studies. The aircraft activity information reflects the analysis year selected for the EIS. The year assumed for the commercial aircraft activity varied for each of the airports: ATL used 2005, ORD used 2002, and PVD used 2004.

While the operations reflect different analysis years, meteorological data for 2002 was used consistently for the analysis. For EDMS, TD-3505 surface weather observations and TD-6201 upper-air soundings for 2002 were obtained from the National Climatic Data Center (NCDC). These data were used by EDMS to estimate the runway that each aircraft would likely have used. In addition, the aircraft performance and emissions computations also use the meteorological data for their calculations. Specifically, the emissions indices (from the International Civil Aviation Organization's Engine Exhaust Emissions Databank 14 [http://www.caa.co.uk/default.aspx?catid=702&pagetype=90], which were based upon standard atmospheric conditions) are adjusted for the airport-specific conditions of ambient temperature, pressure, and humidity.

3.   AIR QUALITY MODELING WITH CMAQ

This study is intended to improve the assessment of aviation emission impacts on local-to-regional air quality using the Community Multiscale Air Quality model, a state-of-the-art, comprehensive, one-atmosphere air quality modeling system that treats gas-phase chemistry, particulate matter (PM), and hazardous air pollutants (HAPs) and air toxics. CMAQ simulates the numerous physical and chemical processes involved in the formation, transport, and destruction of air pollutants. Inputs to the model include emissions estimates (from aircraft and all other anthropogenic and biogenic sources), meteorological fields, and initial condition and boundary condition data. The science in CMAQ is constantly being updated, and the modeling system itself goes through a biennial peer-review process.

We used the MM5-SMOKE-CMAQ modeling system over multiscale modeling domains (Figure 3) at 36-km resolution (national area inside black rectangle) and 12-km resolutions (eastern-U.S. area inside red rectangle) to simulate air quality for the year 2002. (The 4-km domains shown (blue borders) are part of ongoing work, and their results are not presented here.)

We simulated two different emissions scenarios: (1) a base case scenario that included all emissions sources except aviation activities, and (2) a sensitivity scenario that included emissions from commercial aviation activities. The difference in estimated pollutant concentrations between these two simulations indicates the regional air quality impacts of the aircraft emissions that were included in the sensitivity simulation. We used the Carbon Bond 2005 chemical mechanism (Yarwood et al., 2005) for representing the chemical reactions within the modeling system.

3.1 PM Treatment in CMAQ

CMAQ treats particulate matter formation through a modal approach (Binkowski and Roselle, 2003). $PM_{2.5}$ particles are represented by two lognormal distributions for the Aitken and accumulation modes. The Aitken mode includes particles with number mean diameters up to approximately 0.1 μm and the accumulation mode covers the number mean diameters from 0.1 to 2.5 μm. CMAQ treats the following components of $PM_{2.5}$ explicitly in each of these modes: sulfate (ASO4), nitrate (ANO3), ammonium (ANH4), primary organic aerosol (AORG_P), secondary organic aerosol from anthropogenic sources (AORGA), secondary organic aerosol from biogenic sources (AORGB), elemental carbon (AEC), and other unspeciated PM (A25). Primary species are those that are directly emitted, while secondary species are those formed in the atmosphere due to chemical reactions. Note that in the discussions in this paper, we refer to AORG_S, which is the sum of AORGA and AORGB. Also, note that while there are no direct emissions of AORGB from airport emission sources, its concentrations could change due to chemical interactions of aircraft emissions with the background concentrations.

We provide a brief description of the relationship between ASO4, ANO3 and ANH4 as modeled by CMAQ to better understand the formation of each of these secondary inorganic components of $PM_{2.5}$ from aircraft sources, in the presence of background emissions. Sulfate aerosol is formed from the aqueous-phase oxidation of SO_2 to H_2SO_4 in cumulus clouds. This mechanism is very efficient. Gas-phase photochemical production of SO_2 to H_2SO_4 is less efficient than aqueous-phase production. Thus, if sufficient moles of $[NH_4^+]$ are available, the sulfuric acid may be neutralized to ammonium bisulfate (NH_4HSO_4), or ammonium sulfate ($NH_4)_2SO_4$. Sulfate aerosol has a summertime maximum associated with high emissions of SO_2 from electric power production combined with higher photochemical production of OH in the summer. Nitric acid vapor (HNO_3) is formed photochemically from NO_x emissions. If sufficient moles of $[NH_4^+]$ are available, then ammonium nitrate aerosol (NH_4NO_3) can also be formed.

To determine the sufficiency of $[NH_4^+]$, Pinder et al. (2008) define the degree of sulfate neutralization (DSN) as

$$DSN = ([NH_4^+] - [NO_3^-]) / [SO_4^{2-}]$$

where all concentrations are in moles. For DSN = 2, the sulfate is fully neutralized. For DSN > 2, formation of NH_4NO_3 is possible. CMAQ uses this approach for determining ASO4 and ANO3 aerosol concentrations.

3.2 CMAQ Model Evaluation

We evaluated the CMAQ outputs from the base emissions scenario against data from five air quality monitoring networks: Air Quality System (AQS) network, Interagency Monitoring of Protected Visual Environ-ments (IMPROVE) network, Speciation Trends Network (STN), and the Federal Reference Method (FRM) network. The evaluation focused on gas-phase species, and $PM_{2.5}$ and its components when available, for the year 2002 within the 12-km domain. In Figure 4, species EC and OC refer to elemental carbon (AEC in CMAQ), and organic carbon (sum of AORG_P and AORG_S in CMAQ) respectively. The sampling frequency varies across these networks; while FRM, IMPROVE, and STN measure 24-hour averages every third day, AQS reports O_3 concentrations hourly. Brief summary descriptions of these networks can be found in Eder and Yu (2006) and at http://www.epa.gov/ttn/amtic/pmfrm.html.

Figure 4 shows a summary of the model evaluation for $PM_{2.5}$ and its constituent species, and ozone for the base case CMAQ outputs. We have grouped the networks in 2 pairs (AQS and IMPROVE in the first, and STN and FRM in the second) for ease of display. We calculated the mean fractional bias (MFB) and mean fractional error (MFE) values (Boylan and Russell, 2006) for both the 36-km and 12-km domains, and for both $PM_{2.5}$ annual average and quarterly average, against each network. We compute MFB and MFE as follows:

$$MFB = \frac{1}{N} \sum_{i=1}^{N} \frac{\left(C_m - C_o \right)}{\left(\dfrac{C_o + C_m}{2} \right)}$$

$$MFE = \frac{1}{N} \sum_{i=1}^{N} \frac{\left| C_m - C_o \right|}{\left(\dfrac{C_o + C_m}{2} \right)}$$

where C_m is the modeled concentration, C_o is the observed concentration, and N is the total number of observed-modeled pairs. While MFB can vary from -200% to +200%, MFE can range from 0 to +200%. Based upon the definition above for MFE and MFB, less-abundant species are expected to have less stringent goals and criteria for acceptable model performance.

Compared against all three networks, the 12-km CMAQ simulation has a smaller MFE value than the 36-km simulation, with approximately 10% less MFE for each network or time period. Since MFE represents the error relative to the average of observations and model predictions, the smaller MFE values for the 12-km domain suggest that the model better reproduces surface PM$_{2.5}$ concentrations over space and time at this resolution. In general, CMAQ predictions for quarters 1 and 4 (Jan-Mar and Oct-Dec) at each network are associated with larger MFE values than for quarters 2 and 3 (Apr-Jun and Jul-Sep) implying better model performance in the warm season than in the cold season. Among the three networks that measure PM$_{2.5}$, CMAQ tends to predict PM$_{2.5}$ better at STN sites than at FRM sites, while the largest errors occurred at the IMPROVE sites.

Overall, we determined the "acceptability" of our modeling by comparing the MFB and MFE values to other regional-scale modeling studies where the modeled results were evaluated against the same network data. We found that our MFB and MFE results are close to the ranges reported by other modeling studies (U.S. EPA, 2007). The IMPROVE network covers only rural locations; the STN monitors are predominantly deployed at urban sites, and the FRM network includes both rural and urban sites. The model performance at the various networks suggests that CMAQ can predict PM$_{2.5}$ better at urban sites than at rural sites, especially in the cold season.

The calculated MFB for the two simulations and observations displays a similar pattern as the MFE values. The difference between MFE and MFB is that for the former, over-prediction and under-prediction may cancel each other, resulting in a smaller value for the same data pool. The annual MFB values from 12-km are less than that of 36-km (approximately half), indicating that a finer resolution can improve CMAQ model performance for both rural and urban sites. Looking at the speciated components, CMAQ's performance for sulfate is the best, with lowest MFE. Overall, the model performance for this application is qualitatively similar to other regional-scale modeling applications in recent years (Hanna and Benjey, 2006).

3.3 Impacts of Aviation Emissions

We evaluated the air quality impacts of aviation emissions by computing the differences between the CMAQ annual simulations for the base case (no aviation) and the sensitivity case (with aviation). Figure 5 shows the percentage contribution of PM$_{2.5}$ due to commercial aviation emissions at the grid cell that contains the maximum impact. We present this metric for each of the three airports at the two grid resolutions that we modeled. Overall, the impacts seen at 12-km are higher than those at 36-km, due to better resolution of the emissions data in the 12-km cells, and thus less "dilution" of emissions. At the 12-km resolution, ATL and ORD indicate up to a 1.5% contribution, while the contribution from PVD is about 0.1%. Spatial plots of modeled absolute and percent differences in PM$_{2.5}$ at the three airports are shown in Figure 6.

To further understand the relative contributions of the different components of PM$_{2.5}$ to air quality, we present in Figure 7, the absolute value and percentage contributions to total PM$_{2.5}$ from each speciated component that CMAQ currently treats.

As in the PM$_{2.5}$ sensitivity analysis discussed earlier in this section, the current analysis of the contributions of PM$_{2.5}$'s components was also conducted for the grid cell that showed the maximum impact from aviation emissions on an annual basis. As seen in Figure 7, all species except nitrate (ANO3) and secondary organic aerosol (AORGA+AORGB) show positive impacts, i.e., aircraft emissions contribute to increases in aerosol concentrations. While the absolute contribution varies across the three airports, the percent contributions from the individual species are approximately the same at all three airports. The contribution from ANO3 to the change in PM$_{2.5}$ is negative (i.e., ANO3 increases due to the removal of aircraft emissions) at the grid cell where the maximum impact is seen in PM$_{2.5}$. On further analysis, we found that this reduction is compensated for by corresponding increases in ANO3 downwind of the airport, at distances of 150 to 200 km. We illustrate this in Figure 8 by showing how ANO3 and ASO4 change as we move away from the 12-km grid cell that contains the airport, indicated by radius of 0. The term radius here indicates the number of grid cells from the airport grid cell, and for each radius we define a box of concentric grid cells centered on the airport, and then include all grid cells in the outermost ring of that box. Thus, a radius of 1 refers to a box of 3×3 grid cells, 2 refers to a box of 5×5 grid cells centered on the airport, and so on. From the bottom plot in Figure 8, we see that changes in ASO4 concentrations due to aircraft emissions gradually diminish as we move away from the airport grid cell. On the other hand, ANO3 (formed due to secondary reactions) first decreases due to airport emissions closer to the airport grid cell, but then increases as we move further away from the source. We also see positive impacts (increases due to aircraft emissions) in predicted AEC at distances of 100 km from the airport (results not shown).

We repeated the type of analysis shown in Figure 7 on a monthly instead of annual basis, to look at the

effects of seasonal variability on aircraft emissions contributions to ambient $PM_{2.5}$ air quality. Figure 9 shows results from ATL airport emissions in the 12-km modeling. The negative contribution from ANO3 noted earlier in the annual average discussion is seen to a relatively smaller extent during the summer. In the winter months, decreases in ANO3 (due to aircraft emissions) occur when the ANO3 levels are appreciable. The likely cause of ANO3's not changing over ATL in the summer monthly averages is that ASO4 dominates total $PM_{2.5}$ in the eastern U.S. in the summer months, and the additional sulfate from aircraft emissions over the sulfate-rich regime of the ATL airport does not change the ANO3 levels, which are already low.

We next grouped the seven $PM_{2.5}$ species into primary (directly emitted) and secondary (formed in the atmosphere) components of $PM_{2.5}$, within the context of aircraft emissions modeling. The allocation for each species is shown in Table 3. We assign 99% of ASO4 to be secondary in nature, based upon the ratio of SO_2 emissions to primary sulfate emissions. We also assign all of ANO3 and ANH4 to be secondary in nature because there are no primary sources of nitrate emissions from aircraft. AORG_S (the sum of AORGA and AORGB) is all expected to be formed due to secondary reactions. All of AORG_P, AEC, and A25 are expected to be from primary emissions.

Species	Primary	Secondary
ASO4	1%	99%
ANO3	0%	100%
ANH4	0%	100%
AORG_P	100%	0%
AORG_S	0%	100%
AEC	100%	0%
A25	100%	0%

Table 3. Primary and secondary components of $PM_{2.5}$ predictions by CMAQ within the context of aircraft emissions modeling**.**

In Figure 10, we present the percent changes in annual average concentrations of AEC (a primary species) and in ASO4 and ANO3 (both secondary species) due to aircraft emissions from the ATL airport in CMAQ 12-km modeling. While the changes in both AEC and ASO4 are positive in the immediate vicinity of the airport, we see that nitrate aerosol decreases in the same area, but increases as far as about 125-150 km from the airport (shown in orange, northeast of ATL). We see a similar response in the model for both ANO3 and AORG_S (results not shown), i.e., local decreases but downwind increases due to airport emissions. The downwind ANO3 increases in the monthly analyses (results not shown) show impacts at distances of up to 250 km for some months.

Figure 11 shows the percent contribution from primary and secondary $PM_{2.5}$ in the sensitivity scenario,

and in the incremental aircraft contributions (sensitivity minus base). We see that when combined with all background emissions sources, $PM_{2.5}$ from secondary reactions averages slightly above 60% at all three airport grid cells. We compute this metric by focusing on the grid cell that contains the maximum difference between the base case and the sensitivity case. However, when background (non-aviation) contributions are removed, secondary formation from aircraft emissions still contributes from 50% to 60% at all three airports at both grid resolutions. This possibly implies that $PM_{2.5}$ formed from aircraft emissions have similar magnitudes of primary and secondary contributions as the background air, at least at the three airport locations that we studied.

CONCLUSIONS

We have developed EDMS2Inv, a new interface to process commercial aviation emissions in the LTO cycle (up to 10,000 feet) from EDMS through SMOKE, and then through CMAQ. While the FOA3a methodology used to estimate speciated $PM_{2.5}$ emissions is preliminary and likely to be revised, this assessment provides an initial estimate of their impacts. Emissions estimates from EDMS can now be used in a comprehensive air quality model such as CMAQ to assess incremental contributions from aircraft emissions. We have used this interface to model air quality impacts due to aircraft emissions at three major airports: Atlanta – Hartsfield, Chicago – O'Hare and Providence – T.F. Green using two different resolutions of 36 km and 12 km. After establishing that the model is performing reasonably by evaluating it using data from several observational networks, we have used the model in a relative sense to quantify the air quality impacts of aviation emissions, and to distinguish between primary and secondary contributions to $PM_{2.5}$ formation in the vicinity of the three airports. CMAQ model results indicate that aviation emissions can contribute up to 1.5% of annual average $PM_{2.5}$ at ORD. In general, we see higher $PM_{2.5}$ impacts at a 12-km model resolution than at a 36-km resolution. We find that at all three airports, secondary components can contribute up to 60% of the total $PM_{2.5}$ in the modeled locations of maximum contributions from aircraft emissions. Both nitrate and secondary organic aerosol show local decreases near the airports, but increase downwind of the airports, showing the importance of secondary PM formation from aircraft emissions. A higher-resolution model application at 4-km or even finer will likely provide further insights into fine-scale variability and sensitivity of the concentrations due to aircraft emissions in the immediate vicinity of the airports at community scales. Based upon our study at these three airports, we conclude that LTO aircraft emissions from an airport can have air quality impacts at distances of up to 250 km from the airport.

ACKNOWLEDGMENTS

REFERENCES

Baek, B.H., A. Eyth and A. Holland, 2006. Recent Updates to the SMOKE Modeling System, Presented at the 5th Annual CMAS Users Conference, Chapel Hill, NC, October 2006.

Baek, B.H., S. Arunachalam, A. Holland, Z. Adelman, A. Hanna, T. Thrasher, and P. Soucacos (2007) *Development of an Interface for the Emissions Dispersion and Modeling System (EDMS) with the SMOKE Modeling System*. In Proceedings of the 16th Annual Emissions Inventory Conference - "Emissions Inventories: Integration, Analyses and Communication", Raleigh, NC, May 2007. Available at: http://www.epa.gov/ttn/chief/conference/ei16/session1/baek.pdf

Binkowski, F.S. and S.J. Roselle, 2003, Models-3 Community multiscale air quality (CMAQ) model aerosol component, 1 Model description. *J. Geophys. Res.* 108(D6) 4183, doi:10.1029/2001JD001409.

Boylan and Russell, 2006. PM model performance metrics, goals, and criteria for 3-D AQMs, *Atmos. Environ.*, 40 (26): 4946-4959.

Byun, D.W. and J.K.S. Ching, ed., Science Algorithms of the EPA Models-3 Community Multiscale Air Quality (CMAQ) Modeling System, 1999, EPA/600/R-99/030(peer reviewed). [Available from National Exposure Research Laboratory, RTP, NC]

Byun, D.W., and Schere, K.L., 2006. Review of the Governing Equations, Computational Algorithms, and Other Components of the Models-3 Community Multiscale Air Quality (CMAQ) Modeling System. *J. Applied Mechanics Reviews*, 59 (51), 2006.

Cimorelli, A.J., S.G. Perry, A. Venkatram, J.C. Weil, R.J. Paine, R.B. Wilson, R.F. Lee, W.D. Peters, and R.W. Brode, 2005, AERMOD: A Dispersion Model for Industrial Source Applications. Part I: General Model Formulation and Boundary Layer Characterization, *J. Applied Meteorology*, 44. pp 682-693.

Community Multiscale Air Quality (CMAQ) Modeling System, 2008. http://www.cmaq-model.org

Eder, Brian and Shaocai Yu, 2006. A performance evaluation of the 2004 release of Models-3 CMAQ, *Atmos. Environ.* 40 (26): 4811-4824.

EDMS 5.0, 2007. Emissions and Dispersion Modeling System (EDMS) User's Manual, FAA-AEE-0701, Rev4 (06/29/07) Prepared for the Federal Aviation Administration by the CSSI, Inc. Washington, D.C., January 2007.

Federal Register, 1998: Emissions and Dispersion Modeling System (EDMS) Policy for Airport Air Quality Analysis: Interim Guidance to FAA Orders 1050.1D and 5050.4A, 63 Federal Register 70 (30 April 1998), pp. 18068.

Hanna, Adel and William Benjey, Editors, 2006: Special issue on Model Evaluation: Evaluation of Urban and Regional Eulerian Air Quality Models, *Atmos. Environ.*, 40 (26): 4809-5110.

Houyoux, M.R., J.M. Vukovich, C.J. Coats Jr., N.J.M. Wheeler, and P.S. Kasibhatla. 2000. Emission inventory development and processing for the seasonal model for regional air quality (SMRAQ) project. *J. Geophys. Res.* 105(D7):9079-9090.

International Civil Aviation Organization (2007). *Airport Air Quality Guidance Manual*. Document #9889. ICAO Preliminary Edition 2007. Available at: http://www.icao.int/icaonet/dcs/9889/9889_en.pdf

Pinder, R.W., R.L. Dennis, P.V. Bhave, 2008, Observable indicators of the sensitivity of PM2.5 nitrate to emissions reductions-Part I: Derivation of the adjusted gas ratio and applicability at regulatory-relevant time scales, *Atmos. Environ.*, 42, 1275-1286, doi:10.1016/j.atmosenv.2007.10.039.

U.S. Environmental Protection Agency, 2003: User's Guide for the MOBILE 6.1 and MOBILE 6.2, EPA-420/R-03-010, Office of Transportation and Air Quality, August 2003. Available at: http://www.epa.gov/otaq/models/mobile6/420r03010.pdf

U.S. Environmental Protection Agency, 2004: User's Guide for the AMS/EPA AERMOD User's Guide (Version 07026), EPA 454/B-03-001, Research Triangle Park, NC.

U.S. Environmental Protection Agency, 2005: User's Guide for the Final NONROAD Model, EPA-420/R-05-013, Office of Transportation and Air Quality, December 2005. Available at: http://www.epa.gov/otaq/models/nonrdmdl/nonrdmdl2005/420r05013.pdf

U.S. Environmental Protection Agency, 2007: Guidance on the Use of Models and Other Analyses for Demonstrating Attainment of Air Quality Goals for O_3, PM and Regional Haze. EPA-454/B-07-002, OAQPS, RTP, NC, April 2007.

Yarwood, G., S. Rao, M. Yocke, and G. Whitten, 2005: Updates to the Carbon Bond Chemical mechanism: CB05. Final Report to the US EPA, RT-0400675. Available at: http://www.camx.com/publ/pdfs/CB05_Final_Report_120805.pdf
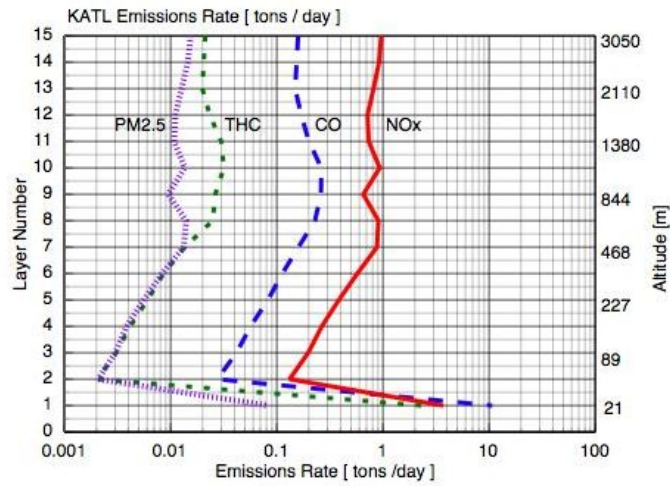
Figure 1. Emissions at ATL airport.
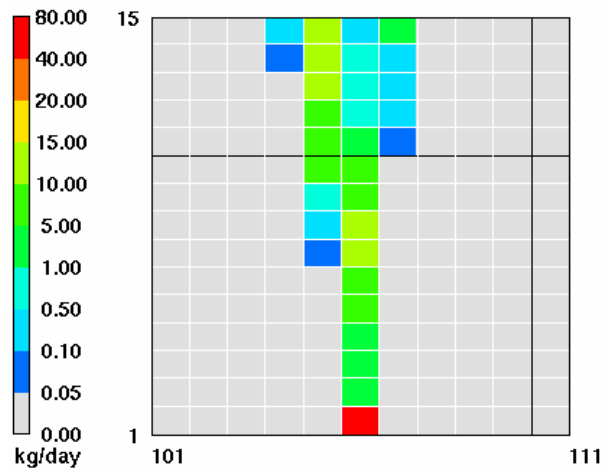
Figure 2. Vertical cross-section of $PM_{2.5}$ emissions at ATL airport.
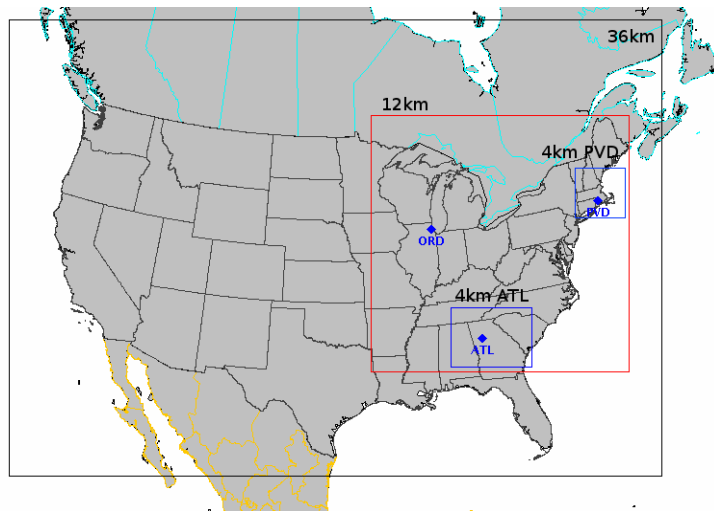
Figure 3. Multiscale CMAQ modeling domains.
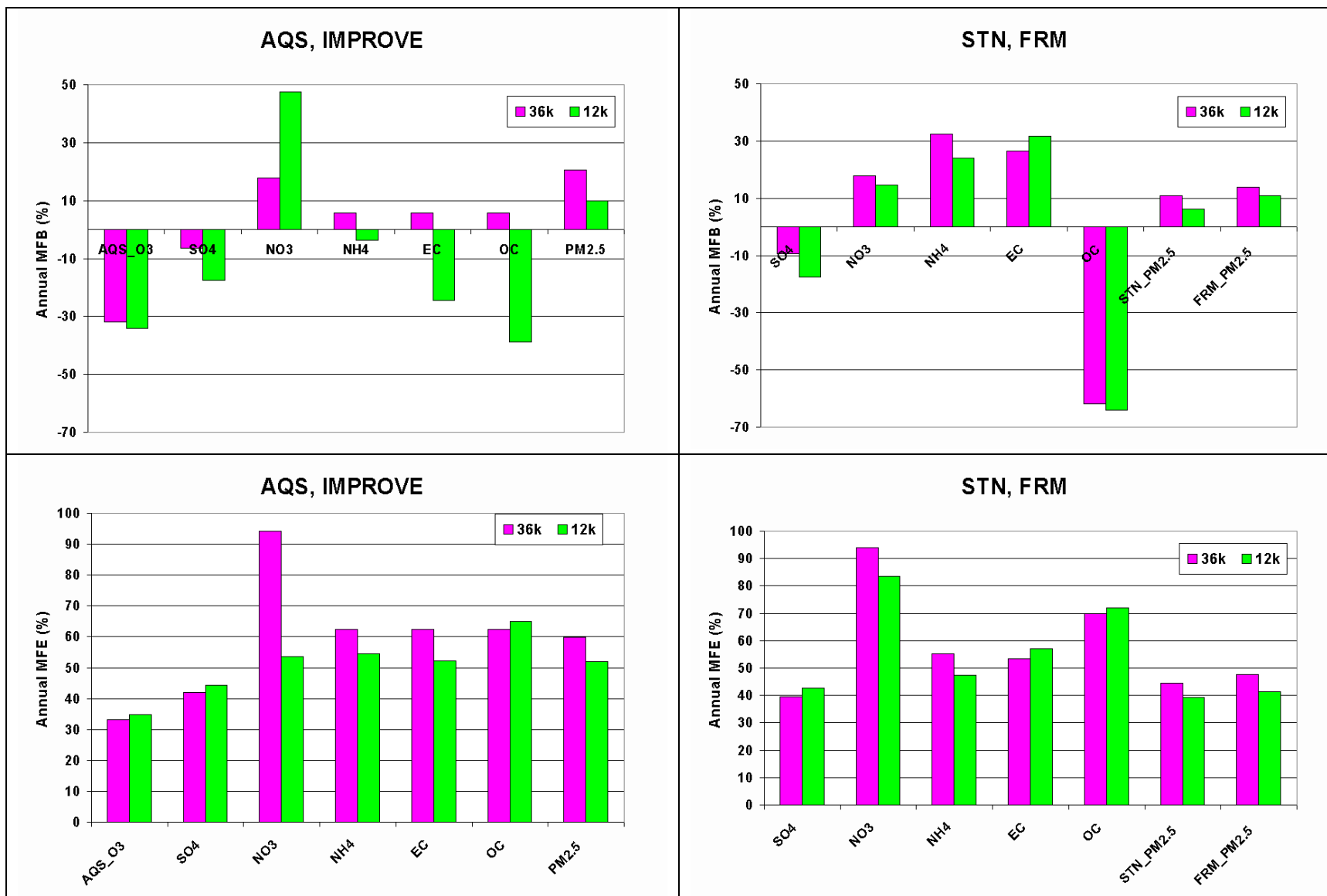
Figure 4. Mean fractional bias (top) and mean fractional error (bottom) computed for CMAQ predictions at 36-km and 12-km compared to various monitoring networks.
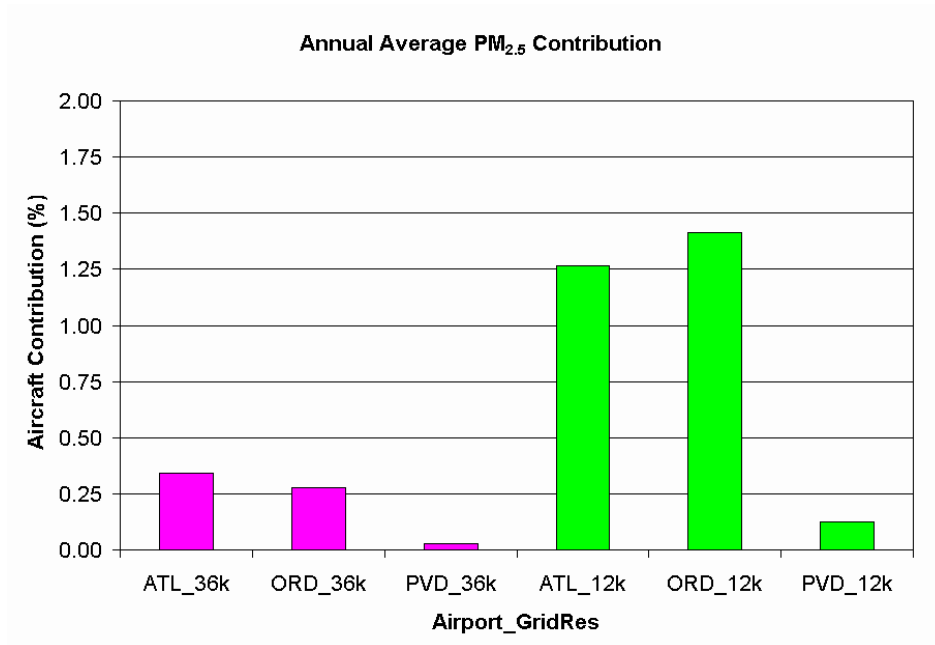
Figure 5. Contribution of aircraft emissions to annual average PM$_{2.5}$ concentrations at the maximum-impact grid cell at each airport, which is the grid cell that contains the airport.
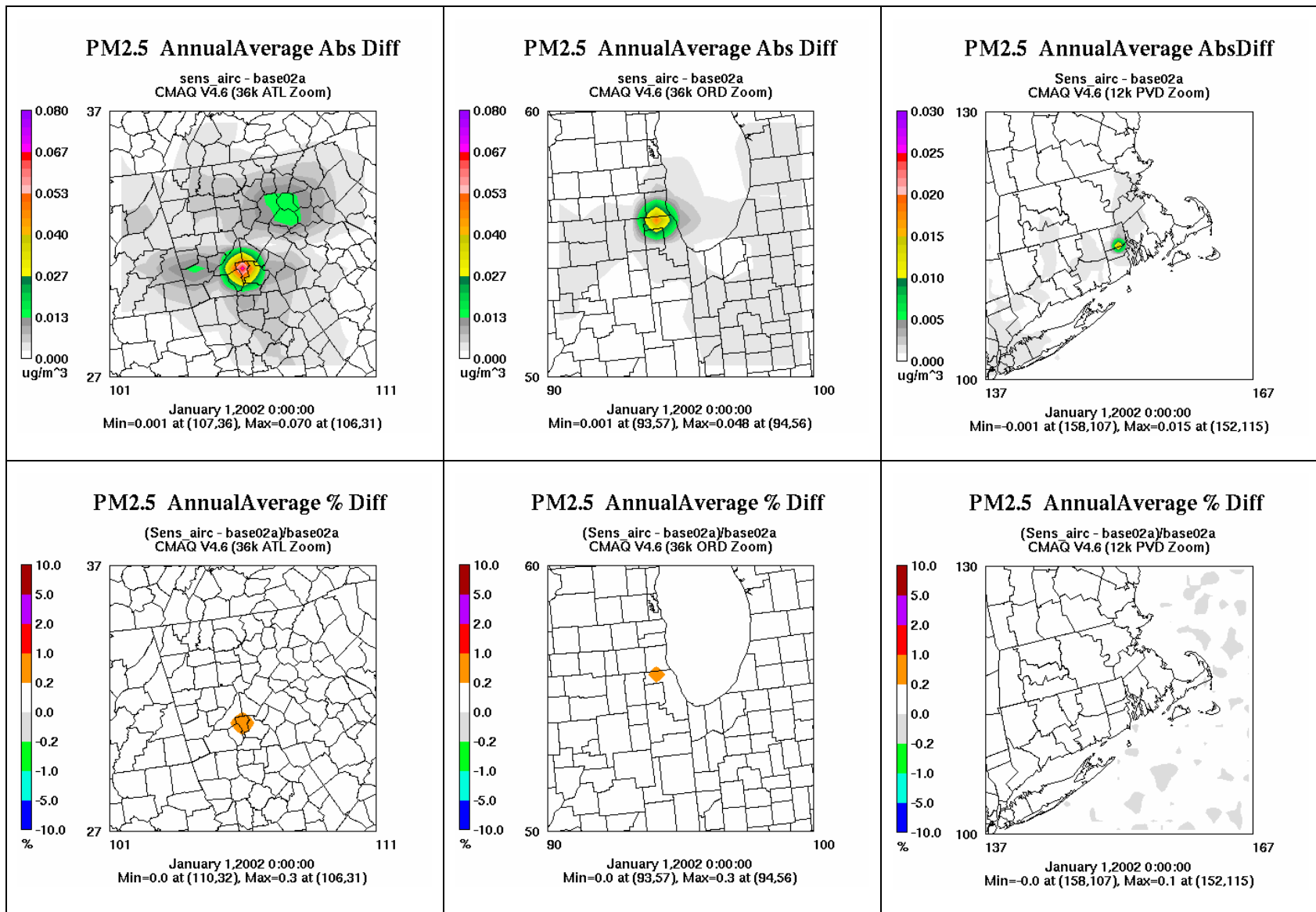
Figure 6. Spatial plots of CMAQ-predicted PM$_{2.5}$ contributions from aircraft emissions for ATL (left), ORD (center), and PVD (right), shown as absolute (top) and percent differences (bottom) in the 36-km resolution. Note that the PVD absolute differences use a different legend maximum than ATL or ORD.

10
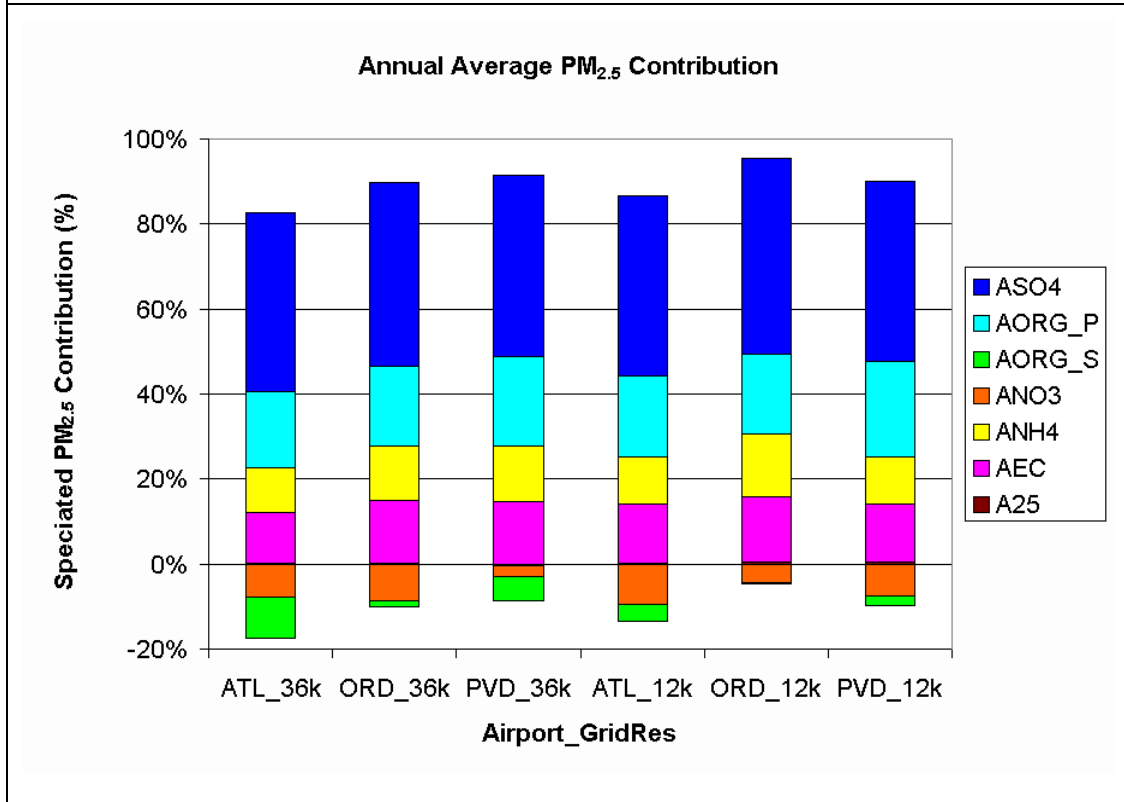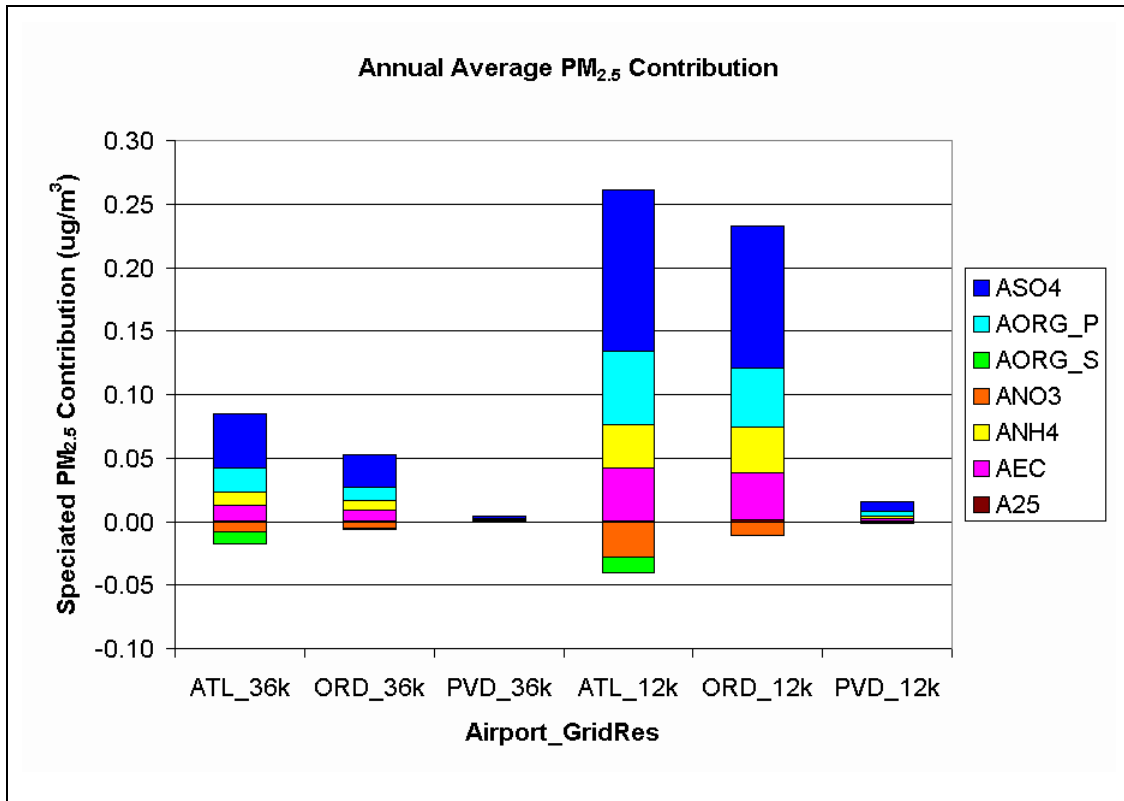
Figure 7. Absolute (top) and percent contribution (bottom) relative to annual average incremental PM$_{2.5}$ from speciated components of PM$_{2.5}$ due to aircraft emissions at each of the three airports at the two model grid resolutions. Analyses performed for the same grid cells shown in Figure 5.
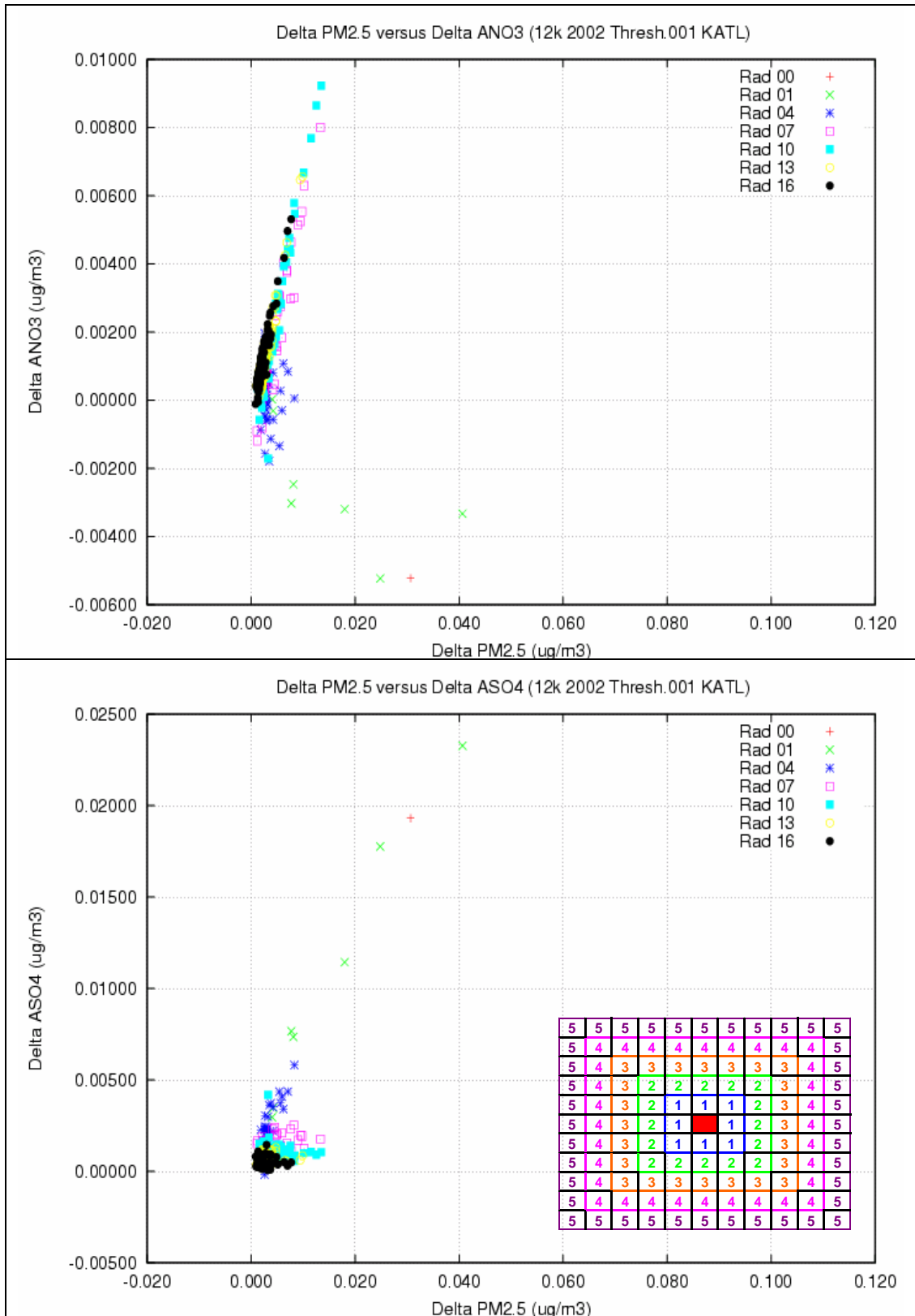
Figure 8. Changes in ANO3 (top) and ASO4 (bottom) compared to changes in PM$_{2.5}$ at increasing distances from the ATL airport grid cell in the 12-km modeling. "Rad" refers to the radius of influence from the grid cell that contains the airport, as shown in the inset in the bottom plot.
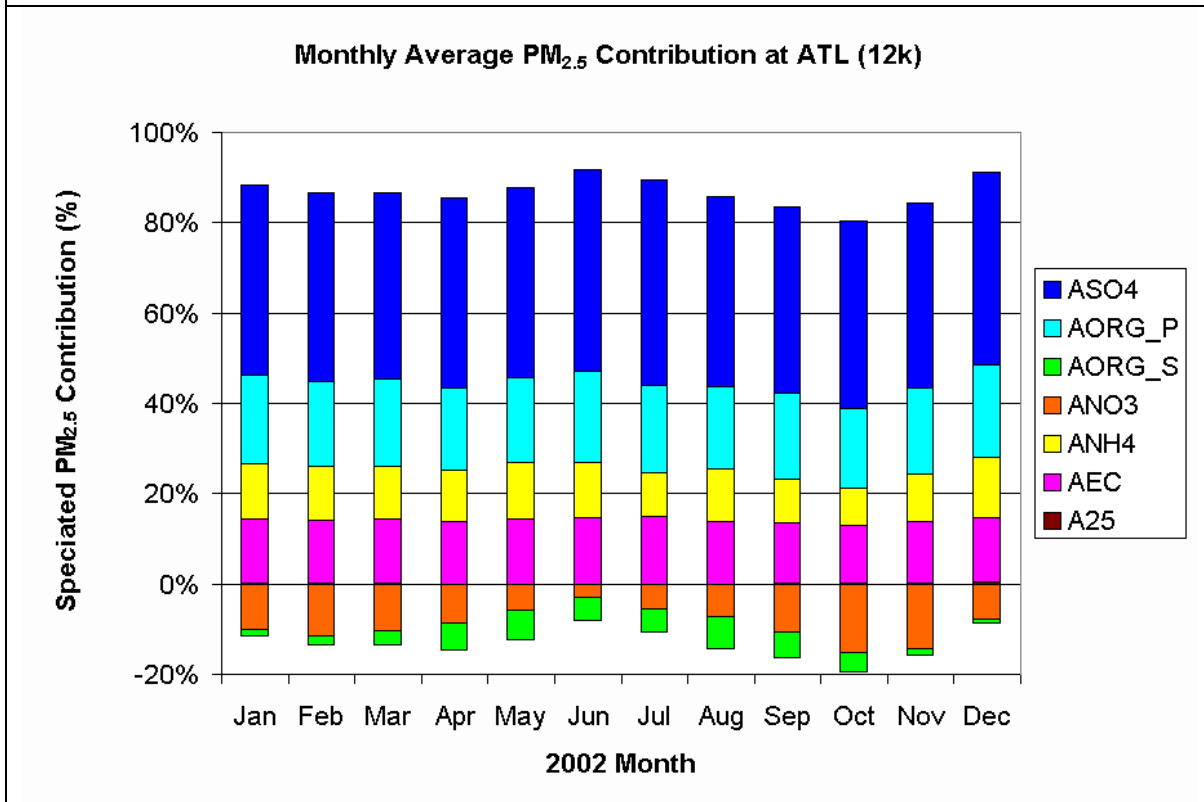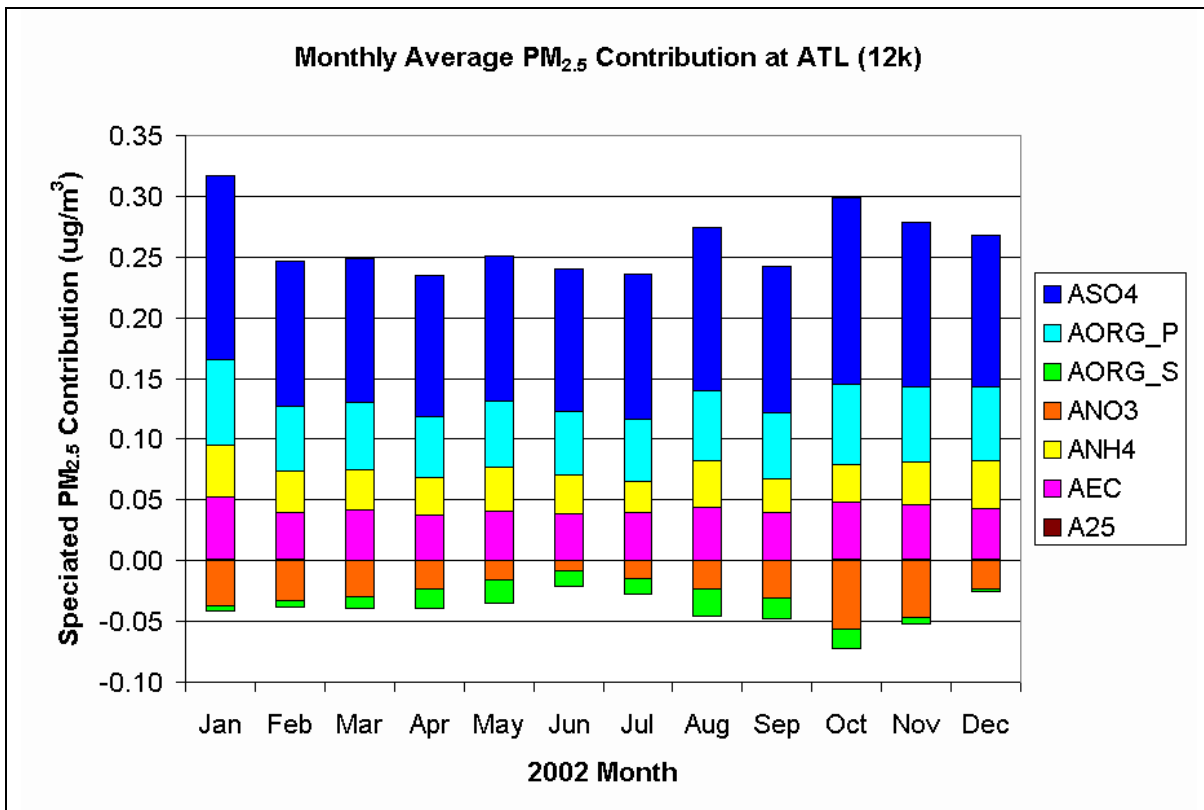
Figure 9. Absolute (top) and percent contribution (bottom) relative to monthly average incremental PM$_{2.5}$ from speciated components of PM$_{2.5}$ due to aircraft emissions at ATL airport from CMAQ 12-km simulations. Analyses performed for the same grid cells shown in Figure 5.
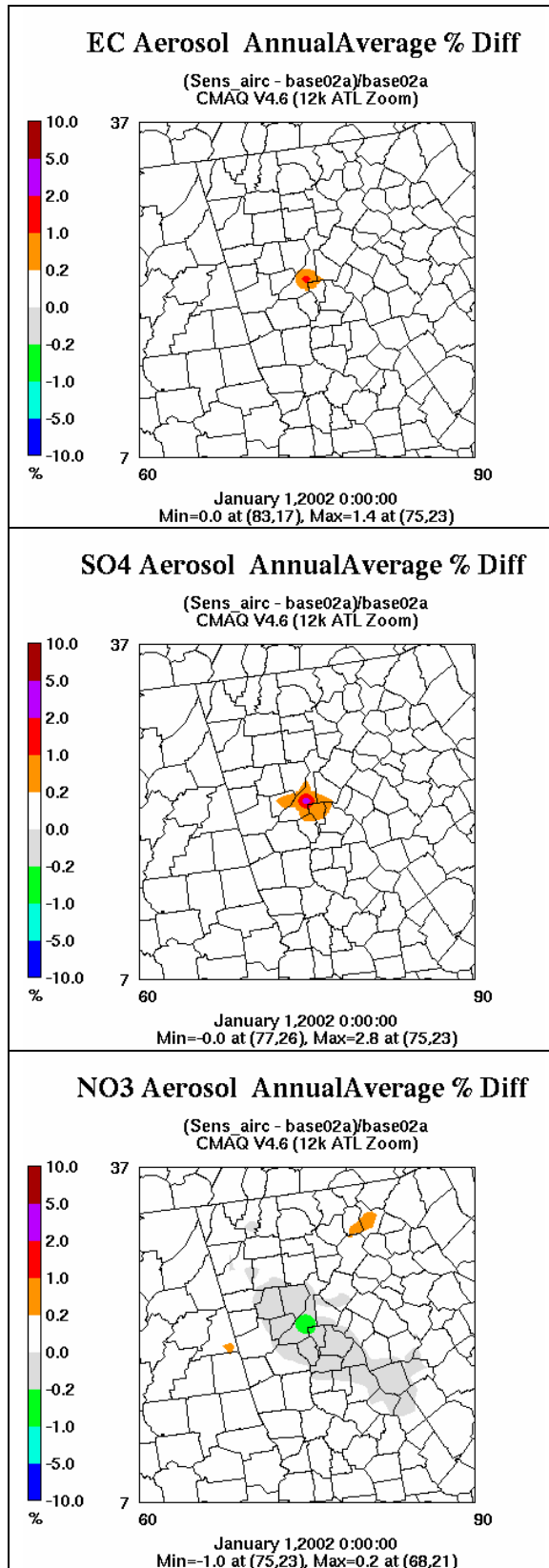
Figure 10. Percent changes in the AEC (top), ASO4 (middle), and ANO3 (bottom) components of PM$_{2.5}$ due to aircraft emissions from ATL in 12-km modeling.
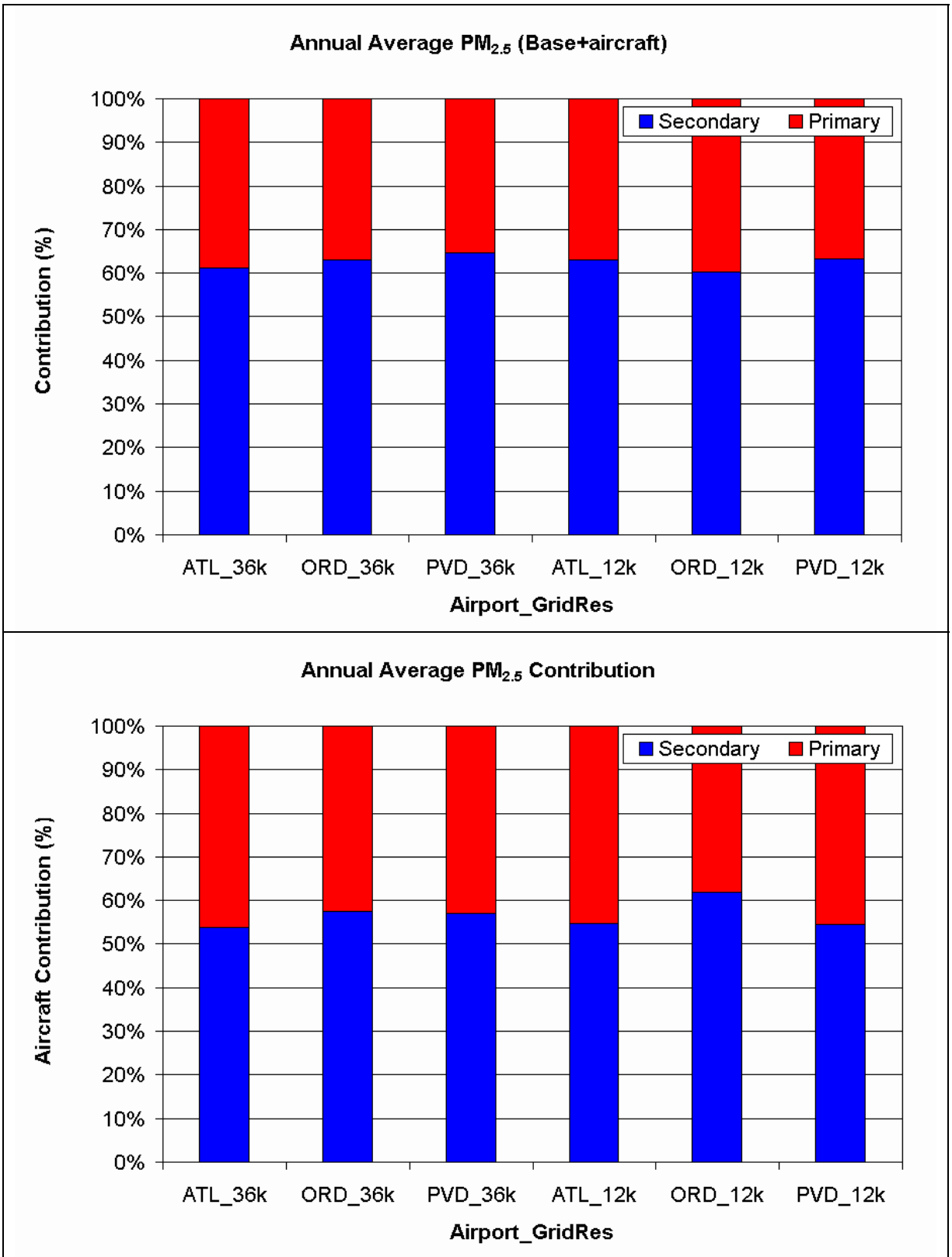
Figure 11. Primary versus secondary contribution to total PM$_{2.5}$ at the three airports in the sensitivity scenario (top) and due to aircraft emissions alone (bottom) at the two model grid resolutions. Analyses performed for the same grid cells shown in Figure 5.